Major and Trace Element Geochemistry of Coals and Intra-Seam Claystones from the Songzao Coalfield, SW China

Lei Zhao [1,2,*], **Colin R. Ward** [3], **David French** [3] and **Ian T. Graham** [3]

[1]   State Key Laboratory of Coal Resources and Safe Mining, China University of Mining and Technology (Beijing), Beijing 100083, China
[2]   College of Geoscience and Survey Engineering, China University of Mining and Technology (Beijing), Beijing 100083, China
[3]   School of Biological, Earth and Environmental Sciences, University of New South Wales, Sydney NSW 2052, Australia; c.ward@unsw.edu.au (C.R.W.); d.french@unsw.edu.au (D.F.); i.graham@unsw.edu.au (I.T.G.)
*   Correspondence: lei.zhao@y7mail.com; Tel.: +86-10-6234-1868

Abstract: Silicic, mafic and alkali intra-seam tonsteins have been known from SW China for a number of years. This paper reports on the geochemical compositions of coals and tonsteins from three seam sections of the Songzao Coalfield, SW China, and evaluates the geological factors responsible for the chemical characteristics of the coal seams, with emphasis on the influence from different types of volcanic ashes. The roof and floor samples of the Songzao coal seams mostly have high TiO_2 contents, consistent with a high TiO_2 content in the detrital sediment input from the source region, namely mafic basalts from the Kangdian Upland on the western margin of the coal basin. The coals from the Songzao Coalfield generally have high ash yields and are highly enriched in trace elements including Nb, Ta, Zr, Hf, rare earth elements (REE), Y, Hg and Se; some variation occurs among different seam sections due to input of geochemically different volcanic ash materials. The geochemistry of the Songzao coals has also been affected by the adjacent tonstein/K-bentonite bands. The relatively immobile elements that are enriched in the altered volcanic ashes also tend to be enriched in the adjacent coal plies, possibly due to leaching by groundwaters. The coals near the alkali tonstein bands in the Tonghua and Yuyang sections of the Songzao Coalfield are mostly high in Nb, Ta, Zr, Hf, Th, U, REE and Y. Coal samples overlying the mafic K-bentonite in the Tonghua section are high in V, Cr, Zn and Cu. The Datong coal, which has neither visible tonstein layers nor obvious volcanogenic minerals, has high TiO_2, V, Cr, Ni, Cu and Zn concentrations in the intervals between the coal plies affected by mafic and alkaline volcanic ashes. This is consistent with the suggestion that a common source material was supplied to the coal basin, derived from the erosion of mafic basaltic rocks of the Kangdian Upland. Although the Songzao coal is generally a high-sulfur coal, most of the chalcophile trace elements show either poor or negative correlations with total iron sulfide contents. The absence of traditional pyrite-metal associations may reflect wide variations in the concentrations of these elements in individual pyrite/marcasite components, or simply poor retention of these elements in the pyrite/marcasite of the relevant coals.

Keywords: geochemistry; coal; rare earth elements; volcanic ash; Late Permian

1. Introduction

The trace element geochemistry of a particular coal is the result of the interaction of the original peaty material with water- and/or air-borne detrital input, and solutions that circulated within the coal basin [1–3], influenced in different ways by the botanical, biochemical and geological factors that acted throughout the long-term process of coal formation [1,4,5]. Among all the factors, incorporation of volcanic ash or influence of volcanic ash layers may have a significant impact not only on the mineralogy, but also on the geochemical characteristics of the individual layers within the coal seams [6,7].

Altered volcanic ash layers are widespread in the Permian strata of southwestern (SW) China [8–10]. Although the geochemistry of tonsteins in the Late Permian coals of SW China indicates an origin from silicic volcanic ash fallout [11], alkali tonsteins that developed in the early part of the Late Permian in SW China have also been reported [10,12,13]. The enrichment of rare metals in coal and its host rocks (e.g., roof and floor strata) in southwestern China, caused by alkali volcanic ashes, has attracted much attention in recent years [3,14–16].

Dai *et al.* [17] indicated that coal from one Songzao coal seam (the No. 11 seam), which contains no visible tonsteins, is significantly enriched in some alkaline elements such as Nb, Ta, Zr, Hf and rare earth elements (REE), and suggested that these geochemical anomalies can be mainly attributed to synsedimentary alkaline volcanic ashes. Another study by Dai *et al.* [18] distinguished three types of tonstein bands (silicic, mafic and alkali) in the Songzao Coalfield based on their distinctive chemical compositions. In a recent study of three individual seam sections in the Songzao Coalfield [19], the modes of occurrence and origin of the mineral assemblages in the volcanic-influenced coal seams were more fully investigated. The present study discusses the modes of occurrence of the trace elements in the coal and associated non-coal strata from the same coal seams. It also provides an opportunity to evaluate the geological factors responsible for the chemical characteristics of coal seams that have been influenced by different types of volcanic ashes. Importantly, the concentrations of rare earth elements and Y (REY, or REE if Y is not included) in the Songzao coals are comparable to those of conventional rare-metal ore deposits and thus the coals are potential raw sources of these metals.

2. Geologic Setting

The Songzao Coalfield is located in SW Chongqing, and encompasses eight different mines (Figure 1). The coal reserves of the Songzao Coalfield are estimated to be 811 Mt as of 2003 [20], accounting for 42.6% of the total coal reserves in Chongqing [18]. The coals of the Songzao Coalfield are mostly high-sulfur anthracites and, in a few cases, medium-sulfur coals (e.g., No. 8 Coal), and are rich in methane. The coalfield is located on the northwestern flanks of the Jiudianya, Jiulongshan and Sangmuchang anticlines.

The Longtan Formation (Late Permian) is the coal-bearing sequence in the coalfield, deposited in a tidal flat system along the western margin of an epicontinental sea [21]. The Longtan Formation consists of limestone, sandstone, silty mudstone, mudstone, coal seams and tuffaceous sediments (Figure 2). The Kangdian Upland to the west was the major sediment source for the coalfield [10,15,22]. The coal-bearing sequence contains 6–11 coal seams, among which the No. 8 coal is workable throughout the entire coalfield, and the Nos. 6, 7, 8, 11 and 12 are locally workable. The Longtan Formation is disconformably underlain by the Maokou Formation, an Early Permian shallow marine limestone unit.
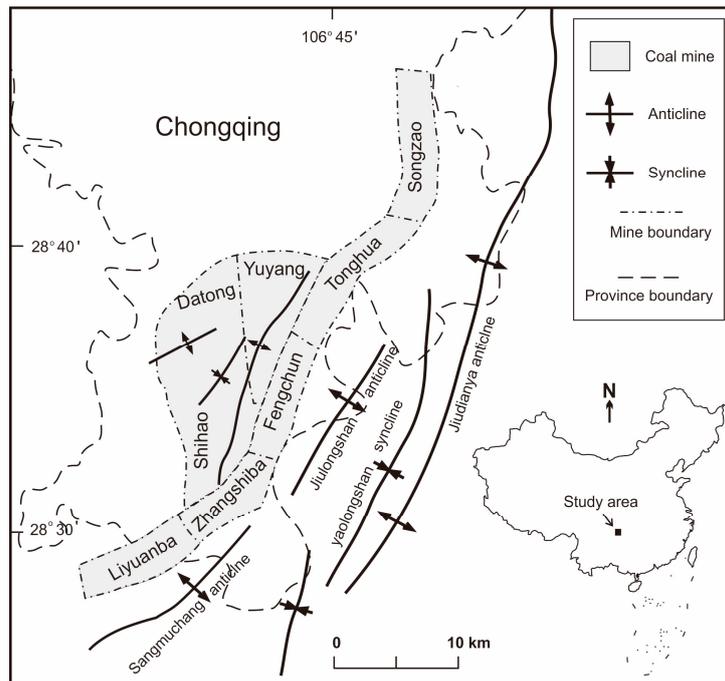
Figure 1. Locality map of the Songzao Coalfield, indicating the mining areas (grey) (after [19]).
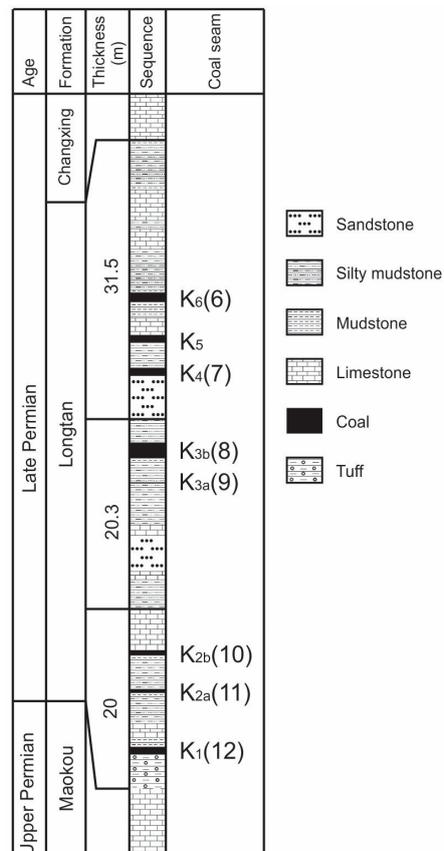
Figure 2. Sedimentary sequence of the Songzao Coalfield, showing the location of the coal seams (after [19]).

3. Sampling and Methods

A total of 24 coal, associated mudrock and intra-seam claystone samples (channel samples) from three seam sections (Datong, Tonghua, and Yuyang) were used for this investigation, as well as for a previous study of the Songzao coal seams [19]. Three series of samples were taken at the underground working faces of the Datong (No. 7 coal), Tonghua (No. k2b coal), and Yuyang (No. 11 coal) mines, respectively (Figure 1).

Each sample was ground to fine powder (about 200 mesh) using a zirconia mill, and split into representative portions for further analyses. All the coal samples were ashed at 815 °C, following procedures described by Standards Australia [23]; the resultant ashes and the ground non-coal samples were analyzed by X-ray fluorescence (XRF) spectrometry to determine the concentrations of major elements. The coal samples were also subjected to low-temperature oxygen-plasma ashing and both the coal mineral residues (low-temperature ash or LTA) and the non-coal rock samples analyzed by X-ray diffraction (XRD) techniques, using Siroquant software (Sietronics Pty Ltd., Belconnen, ACT, Australia) for quantitative mineralogical analysis. Samples were also examined in polished section using scanning electron microscopy combined with energy-dispersive spectrometry (SEM-EDS) techniques, to identify the modes of mineral occurrence. The XRD, XRF and SEM procedures are discussed further by Zhao *et al.* [19].

Concentrations of most trace elements in the coal and rock samples were determined by inductively coupled plasma-mass spectrometry/ optical emission spectrometry (ICP-MS/OES). Prior to the ICP-MS/OES analysis, two separate digestion procedures were carried-out, to accomplish total decomposition of the samples and to ensure that the total element content in each sample was reflected in the resultant digests. One procedure involved ashing the coal and rock samples at 450 °C. The ashes were then subjected to microwave dissolution in a mixed acid (HCl, HF and HNO_3). The other procedure involved fusion with a mixture of lithium tetraborate ($Li_2B_4O_7$) and lithium metaborate ($LiBO_2$) flux, done on the relevant samples without an ashing process. Following microwave-assisted acid digestion or borate fusion, the resultant digests were analyzed by ICP-MS/OES, and the determined values were calculated as concentrations in the original coal or rock samples. ICP-MS techniques for determination of trace elements in coal and associated rock samples have been discussed by Dai *et al.* [18]. Arsenic and selenium in the samples were analyzed using the ICP-MS technique, following the method described by Li *et al.* [24].

Fluorine in the samples was determined using a pyrohydrolysis/fluoride ion-selective electrode technique, following procedures described by Chinese National Standard GB/T 4633-1997 [25]. Mercury in the samples was analyzed using a Milestone DMA-80 Hg analyzer (Milestone, Milan, Italy); the detection limit of Hg is 0.005 ng and the linearity of the calibration is in the range 0–1000 ng.

4. Results and Discussion

4.1. Coal Characteristics

Table 1 lists the proximate analysis, total and pyritic sulfur contents of selected samples, and the mean maximum vitrinite reflectance value of the coal samples, as well as clay mineralogy obtained from the <2 μm fractions of all coal LTAs and non-coal strata, as discussed by Zhao *et al.* [19]. The Songzao coals have medium to high ash yield and varying sulfur percentages. The coal is mainly semi-anthracite under the classification of the American Society for Testing and Materials (ASTM), based on the volatile matter value and fixed carbon percentages [26].

Table 1. Proximate analysis, total and pyritic sulfur (selected samples), mean maximum vitrinite reflectance value of the Songzao coal samples (%, air-dried basis, unless indicated), as well as oriented-aggregate X-ray diffraction (XRD) data for clay minerals (wt % of <2 μm fraction) in all coal low-temperature ash (LTAs) and non-coal strata (all data from Zhao *et al.*, 2013 [19]).

Sample	Thickness (cm)	Ash Yield	VM_{daf}	FC_{daf}	Total Sulfur	Pyritic Sulfur	$R_{v,max}$	Clay Minerals		
								Kao (+ Chl)	I	E
dt-7-0	-	-	-	-	-	-	-	71	7	23
dt-7-1	15	20.6	10.0	90.0	6.73	5.00	2.22	86	0	14
dt-7-2	22	18.2	10.3	89.7	4.89	-	2.17	100	0	0
dt-7-3	12	19.4	9.4	90.6	4.62	4.10	2.36	86	0	14
dt-7-4	24	23.2	8.0	92.0	3.73	-	2.33	78	4	18
dt-7-5	20	35.4	9.5	90.5	3.21	-	2.29	80	7	12
dt-7-6	-	-	-	-	-	-	-	69	26	5
th-k2b-0	-	-	-	-	-	-	-	11	25	64
th-k2b-1	30	32.3	8.1	91.9	2.97	-	2.40	76	1	22
th-k2b-2	7	43.7	6.9	93.1	0.78	-	2.42	89	0	10
th-k2b-3	-	-	-	-	-	-	-	22	28	50
th-k2b-4	11	36.6	11.1	88.1	10.10	-	2.30	78	0	22
th-k2b-5	-	-	-	-	-	-	-	66	10	25
th-k2b-6	6	36.6	10.7	89.3	1.22	-	2.42	90	0	10
th-k2b-7	-	-	-	-	-	-	-	40	35	26
yy-11-0	-	-	-	-	-	-	-	27	45	28
yy-11-1	10	35.9	7.0	93.0	8.11	-	2.09	100	0	0
yy-11-2	7	24.1	8.9	91.2	8.13	-	2.25	100	0	0
yy-11-3	7	24.2	10.0	90.0	13.39	11.0	2.31	100	0	0
yy-11-4	14	23.6	9.5	90.5	10.08	8.50	2.40	100	0	0
yy-11-5	8	41.3	7.7	92.3	3.03	2.40	2.28	93	0	7
yy-11-6	-	-	-	-	-	-	-	88	0	12
yy-11-7	11	31.5	8.4	91.6	1.64	-	2.25	93	0	7
yy-11-8	-	-	-	-	-	-	-	41	26	33

VM, volatile matter; FC, fixed carbon; daf, dry ash-free basis; $R_{v,max}$, mean maximum vitrinite reflectance; Kao, kaolinite; Chl, chlorite; I, illite; E, expandable clays.

According to Lyons *et al.* [27] and Spears [28], volcanogenic claystones are referred to as tonsteins or K-bentonites, respectively, when kaolinite or mixed-layer illite/smectite (I/S) exceeds 50% of the respective clay mineral assemblages. Claystone sample th-k2b-3 is thus a K-bentonite, and claystones th-k2b-5 and yy-11-6, which have >50% kaolinite, are tonsteins.

4.2. Geochemical Associations in Coal Samples

Major and trace element data for the Songzao coal and non-coal samples are given in Table 2. In general, the Songzao coals have relatively high concentrations of most trace elements compared to the respective averages for worldwide coals [29]. This is especially so for the lithophile elements, which usually show a positive correlation with the ash yield of coal [30,31]. The relationship between the mineralogical data and major-element ash chemistry for the Songzao coals has been previously evaluated by Zhao *et al.* [19].

The geochemical results from the Songzao coal samples were evaluated using cluster analysis, to identify groups of associated trace elements and major element oxides. The major element oxide percentages determined by XRF analysis of the coal ashes were recalculated to give the percentages of those oxides in the whole coal, before the cluster analysis was undertaken.

Hierarchical clustering was performed using Pearson correlation coefficients. The likely organic/mineral affinity of the elements in the Songzao coals is indicated by the statistical correlation of the different trace element concentrations with the ash yield. Elements with a strong inorganic affinity would be expected to show a positive correlation to the ash percentage, and those with a strong organic affinity would show a negative correlation. Elements that are the most strongly correlated are linked first, and then elements or element groups with decreasing correlation, until a complete dendrogram is achieved.

Table 2. Major oxide and trace element analyses of the Songzao coal and associated non-coal samples from three seam sections (Major oxides in wt %, trace elements in ppm, unless otherwise indicated. All data are on a whole-coal basis. Major element oxides recalculated from the data by X-ray fluorescence (XRF) analysis. Trace elements determined by ICP-MS/OES analysis).

Sample	Major Element Oxide (wt %) and Trace Element (ppm)																						
	SiO_2	Al_2O_3	TiO_2	Fe_2O_3	MgO	CaO	Na_2O	K_2O	P_2O_5	MnO	Li	Be	F	Sc	V	Cr	Co	Ni	Cu	Zn	Ga	Ge	As
dt-7-0	36.9	24.9	3.82	9.04	0.66	0.50	0.870	1.042	0.226	0.148	197	4.9	354	62.0	360	168	65.4	101	192	213	44.0	2.2	9.3
dt-7-1	6.9	4.8	0.30	7.35	0.06	0.44	0.079	0.073	0.048	0.006	57	2.1	71	10.0	47	22	11.6	19	35	12	8.0	1.7	3.9
dt-7-2	5.3	4.0	0.20	5.63	0.08	1.77	0.040	0.056	0.029	0.011	57	1.6	64	11.4	108	23	15.8	15	60	16	6.1	2.0	3.0
dt-7-3	7.1	5.0	0.26	5.11	0.11	1.11	0.053	0.118	0.011	0.008	69	1.4	41	11.5	97	24	20.4	23	56	49	8.6	1.7	2.9
dt-7-4	10.2	6.8	0.68	3.99	0.13	0.52	0.114	0.255	0.015	0.004	70	6.0	76	18.9	157	56	23.1	41	98	251	10.1	1.1	4.4
dt-7-5	17.0	7.6	0.59	4.36	0.32	3.37	0.108	0.351	0.027	0.015	107	1.4	96	25.2	154	50	35.5	213	71	34	13.0	1.1	2.5
dt-7-6	42.1	31.5	5.99	1.41	0.36	0.21	1.697	1.203	0.067	0.010	235	4.6	309	65.5	433	297	22.9	55	152	85	51.4	2.7	<1
th-k2b-0	41.3	16.1	1.79	11.19	0.72	0.64	0.907	1.965	0.114	0.050	53	5.6	1697	47.6	279	137	51.5	125	88	81	31.2	1.8	36.7
th-k2b-1	15.6	7.7	0.51	4.20	0.72	1.81	0.181	0.343	0.037	0.020	80	3.5	533	33.7	335	65	43.3	91	334	24	14.6	1.7	2.9
th-k2b-2	23.1	15.2	1.79	1.00	0.25	0.75	0.290	0.395	0.056	0.006	185	4.2	536	48.4	457	103	9.6	39	305	43	24.5	2.5	0.8
th-k2b-3	39.6	28.6	4.09	4.17	0.53	0.25	2.016	1.300	0.051	0.025	186	12.8	1014	65.8	385	201	32.8	140	260	110	53.3	4.5	1.0
th-k2b-4	8.3	4.9	0.32	13.80	1.46	3.36	0.145	0.177	0.040	0.033	50	2.2	326	19.5	170	32	18.7	76	81	42	9.0	1.1	5.4
th-k2b-5	42.5	31.0	1.44	0.88	0.55	0.22	1.205	1.375	0.031	0.007	211	9.4	1288	33.6	27	8	3.5	34	<2	45	75.3	3.1	<1
th-k2b-6	13.7	7.2	0.44	7.24	1.71	3.70	0.080	0.174	0.067	0.040	97	1.6	365	26.0	160	41	25.7	70	69	48	12.7	1.5	5.2
th-k2b-7	42.2	31.4	5.28	2.39	0.65	0.24	2.188	1.359	0.050	0.014	233	6.8	1184	60.9	502	234	21.7	111	124	86	59.1	4.4	<1
yy-11-0	50.4	20.3	1.84	5.26	0.89	0.28	1.260	2.459	0.112	0.029	39	5.8	1635	45.1	182	39	25.6	42	144	119	39.8	2.0	2.3
yy-11-1	21.6	2.3	0.37	10.56	0.02	0.12	0.014	0.040	0.012	0.011	18	17.4	58	16.6	33	15	15.4	28	18	13	5.6	3.8	4.8
yy-11-2	11.0	2.1	0.28	9.17	0.06	0.61	0.022	0.041	0.007	0.005	15	6.8	70	10.2	24	15	17.2	22	17	10	6.2	3.6	5.3
yy-11-3	5.1	2.1	0.17	13.49	0.09	0.92	0.019	0.024	0.009	0.006	14	7.8	69	6.1	18	11	13.1	6	23	11	6.7	3.4	6.9
yy-11-4	7.7	3.9	0.27	13.91	0.15	0.96	0.015	0.059	0.019	0.009	30	5.9	98	6.7	22	15	107	68	92	11	8.5	3.7	6.9
yy-11-5	21.0	13.6	0.59	3.53	0.30	0.95	0.186	0.334	0.027	0.010	110	4.9	530	16.5	26	14	4.2	10	7	42	26.5	3.8	2.3
yy-11-6	41.6	31.8	1.42	0.37	0.36	0.20	0.575	0.809	0.018	0.008	251	14.0	1225	27.7	11	5	9.8	6	<2	20	62.4	7.9	<1
yy-11-7	16.8	8.0	0.24	2.26	0.42	2.17	0.093	0.159	0.050	0.021	59	7.3	343	15.1	23	13	3.7	16	3	9	12.2	2.0	1.6
yy-11-8	43.0	25.6	2.94	4.81	0.96	0.31	0.739	2.949	0.073	0.024	75	9.3	2587	52.8	300	89	30.6	65	123	182	55.0	3.4	16.6

Table 2. *Cont.*

Sample	Trace Element (ppm)																						
	Se	Rb	Cs	Sr	Y	Zr	Nb	Mo	Ag	Cd	Sn	Sb	Te	Ba	Hf	Ta	W	Hg (ppb)	Tl	Pb	Bi	Th	U
dt-7-0	3.43	24.05	1.94	613	56	536	69.0	1.3	1.34	0.22	4.65	0.70	1.14	216.9	26.7	6.48	1.76	108	<0.02	16.6	0.18	20.6	6.1
dt-7-1	8.63	1.67	0.18	206	13	56	5.6	1.7	0.12	0.09	1.06	0.47	0.16	18.2	3.1	0.50	0.37	459	0.06	16.9	0.35	6.3	2.5
dt-7-2	9.17	1.51	0.18	213	18	49	3.8	1.0	0.10	0.10	1.00	0.53	0.23	14.6	3.2	0.48	0.21	450	0.03	13.8	0.33	6.7	1.9
dt-7-3	12.32	3.16	0.44	133	17	67	10.0	2.4	0.16	0.46	1.79	1.05	0.29	17.6	4.3	0.64	1.09	852	0.02	16.5	0.48	10.3	2.3
dt-7-4	15.30	6.06	0.73	120	23	99	10.4	1.7	0.22	0.58	1.65	0.86	0.11	36.6	6.2	0.96	0.54	1102	0.04	46.6	0.32	10.8	2.6
dt-7-5	13.05	8.48	1.07	292	32	221	12.4	1.5	0.35	0.22	3.31	1.14	0.20	45.1	9.1	1.34	0.49	679	0.06	10.1	0.48	11.8	3.7
dt-7-6	6.46	21.32	1.17	841	49	611	107.5	1.5	1.69	0.22	5.85	0.78	1.06	266.2	30.9	8.25	2.24	855	<0.02	6.8	0.13	25.1	5.6
th-k2b-0	8.21	45.79	2.94	719	38	521	73.0	20.4	1.47	0.34	5.96	1.27	0.80	173.3	28.5	7.64	0.97	414	0.03	21.7	0.30	25.2	10.2
th-k2b-1	10.81	7.22	1.00	285	77	162	20.2	2.0	0.81	0.25	4.77	0.50	0.36	35.0	9.9	1.83	0.58	906	0.07	22.8	0.38	17.6	4.2
th-k2b-2	5.28	8.54	1.09	301	42	283	51.0	1.2	0.92	0.15	4.12	0.39	0.18	57.3	17.2	4.01	1.56	196	0.03	10.0	0.42	23.0	4.6
th-k2b-3	10.64	22.92	1.44	1134	37	581	82.8	2.2	1.60	0.31	6.18	1.15	0.58	214.5	30.4	7.35	3.17	369	0.05	30.2	0.17	21.5	4.7
th-k2b-4	15.62	3.68	0.53	311	70	334	41.6	3.5	0.76	0.39	4.94	0.86	0.29	20.9	15.1	1.42	0.80	781	0.03	23.3	0.41	8.3	4.3
th-k2b-5	3.29	23.10	1.65	825	37	857	355.6	1.1	5.16	0.34	13.16	0.75	0.70	183.8	66.8	31.71	1.87	457	<0.02	9.2	0.63	76.8	9.3
th-k2b-6	11.93	3.97	0.59	432	101	665	38.1	6.0	0.76	0.34	5.69	0.78	0.41	23.7	26.6	2.04	1.16	361	0.03	11.7	0.39	13.7	5.0
th-k2b-7	3.07	23.97	1.60	971	53	739	106.6	2.7	1.67	0.29	6.93	0.72	0.27	204.1	36.1	7.79	3.07	148	0.03	10.6	0.19	24.7	5.0
yy-11-0	9.70	43.50	2.55	729	41	531	88.7	1.5	1.47	0.22	5.71	0.92	0.28	167.5	30.5	7.00	2.89	196	0.03	22.8	0.07	25.8	4.4
yy-11-1	7.88	0.73	0.14	72	13	106	7.3	3.2	0.17	0.09	1.44	0.43	0.15	9.1	5.6	0.91	0.70	917	0.50	8.9	0.24	4.9	2.9
yy-11-2	12.05	0.76	0.14	99	14	85	6.4	3.5	0.14	0.06	1.25	0.39	<0.1	9.0	4.6	0.77	0.20	764	0.46	7.8	0.18	5.8	1.8
yy-11-3	14.01	0.51	0.10	112	16	68	4.9	5.8	0.12	0.12	0.87	0.43	<0.1	5.2	3.7	0.64	0.38	599	0.37	20.0	0.09	4.0	1.3
yy-11-4	12.57	1.11	0.20	95	22	123	11.9	4.1	0.21	0.11	1.26	0.41	<0.1	7.4	6.6	1.29	0.13	861	0.57	16.6	0.13	7.1	2.6
yy-11-5	7.06	6.04	0.99	239	56	537	134.2	2.5	2.58	0.28	8.55	0.55	0.18	37.5	32.2	12.69	1.55	443	0.11	21.0	0.30	27.2	6.5
yy-11-6	0.24	12.20	1.98	418	40	529	403.8	2.5	6.28	0.13	14.48	0.78	0.43	84.4	31.7	33.27	4.22	93	<0.02	1.2	0.17	29.2	4.8
yy-11-7	6.28	3.72	0.65	204	75	773	57.4	1.8	1.12	0.16	6.12	0.36	0.23	19.6	37.8	3.82	0.24	203	0.02	8.2	0.11	23.4	7.8
yy-11-8	10.85	57.98	4.01	794	69	1068	155.7	3.4	2.46	0.40	8.60	1.01	0.47	174.5	50.3	12.22	7.57	175	0.09	30.0	0.24	37.7	10.3

Major element data from *Zhao et al.* [19].

Associations of elements in the Songzao coals are broadly indicated by the resulting dendrogram (Figure 3). The six main groups, and also the statistical correlation coefficients between selected elements and ash yield, are shown in Table 3. Apart from the inter-correlation among elements in the same group, each group may also include elements of different sub-groups that have different correlations with Al_2O_3, CaO, or the abundance of particular minerals in the coals. The possible modes of occurrence of the different elements can be inferred based on the correlation of their concentrations with particular mineralogical abundances, with both of the element and mineral contents recalculated to a whole-coal basis prior to the correlation analysis.
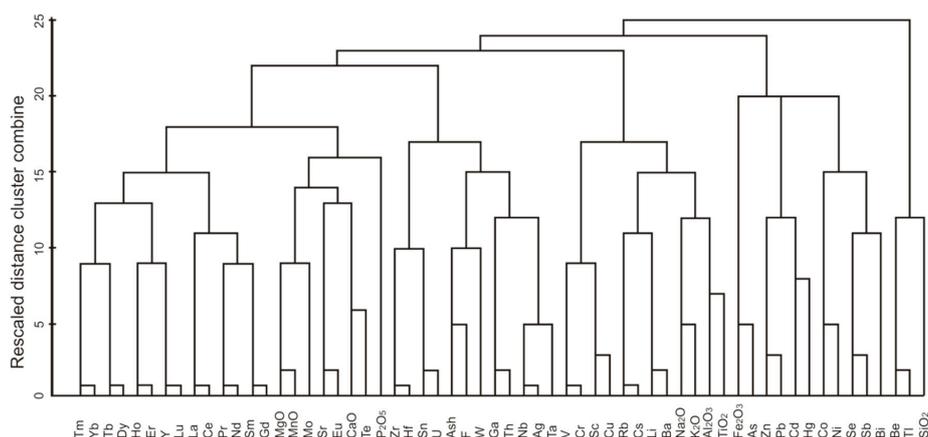
Figure 3. Dendrogram developed from cluster analysis on the geochemical data of the coals from three seam sections in the Songzao Coalfield (cluster method, centroid clustering; interval, Pearson correlation; transform values, maximum magnitude of 1).

Table 3. Broad classification of elements according to the results from cluster analysis, and also correlation coefficients (*R*, in parentheses) between concentrations of individual elements (E) and Al_2O_3, CaO or the sum of pyrite and marcasite in the coals.

Group	Element (Correlation Coefficient)	Element or Mineral to which the Elements in the Group Correlate
Group A	Al_2O_3 (1), TiO_2 (0.79), Rb (0.82), Cs (0.86), Li (0.92), Ba (0.87), Na_2O (0.9), K_2O (0.86), Sc (0.73), Cr (0.63), V(0.59), Cu (0.47)	$R(E-Al_2O_3)$
Group B	Hf (0.63), Sn (0.72), U (0.69), F (0.8), W (0.74), Ga (0.97), Th (0.91), Nb (0.75), Ag (0.76), Ta (0.73), Zr (0.5)	$R(E-Al_2O_3)$
Group C	Tm (0.44), Yb (0.47), Tb (0.52), Dy (0.5), Ho (0.47), Er (0.49), Y (0.46), Lu (0.43), La (0.59), Ce (0.57), Pr (0.55), Nd (0.53), Sm (0.51), Gd (0.59)	$R(E-Al_2O_3)$
Group D	CaO (1), MgO (0.8), MnO (0.86), Sr (0.77), Eu (0.42), Te (0.66), P_2O_5 (0.52), Mo (0.19)	$R(E-CaO)$
Group E	Fe_2O_3 (0.95), As (0.89), Hg (0.32), Zn (−0.32), Pb (−0.06), Cd (−0.37), Co (0.35), Ni (−0.17), Se (0.43), Sb (−0.3), Bi (−0.58)	$R(E-(Py + Mar))$
Group F	Be (−0.28), Tl (−0.16), SiO_2 (0.84)	$R(E-Al_2O_3)$

Group A includes TiO_2, V, Cr, Sc, Cu, Rb, Cs, Li, Ba, Na_2O, K_2O and Al_2O_3. With the exception of Sc, Cr, V and Cu, elements in Group A are all strongly correlated with Al_2O_3, with high correlation coefficients (*R* > 0.79). On the other hand, slightly lower correlation coefficients generally exist between these elements and the ash yield. Most of the elements in this group probably have a common source.

Group B includes Zr, Hf, Sn, U, F, W, Ga, Th, Nb, Ag and Ta. With the exception of Ga and Th, these elements have relatively strong correlations with Al_2O_3, with correlation coefficients in the range

of 0.5–0.79. Ga and Th stand out in this group, as they have greater affinity with Al_2O_3 than other elements ($R = 0.97$ and 0.91, respectively). The comparison of Ga against Al_2O_3 is shown in Figure 4A. Ga and Th are clustered in this group because of their close association with other elements in the group, for example Th with U ($R = 0.87$), and Ga with Nb ($R = 0.83$). The elements in this group also probably have a common source.

Group C includes all the REE except Eu. The correlation coefficients between the REE in this group and the Al_2O_3 concentration in the coals are in the range of 0.44 to 0.59. Higher correlation coefficients generally exist between these elements and the ash yield ($R = 0.6$–0.68). This may indicate that the REE are mainly moderately associated with ash yield in the Songzao coals.
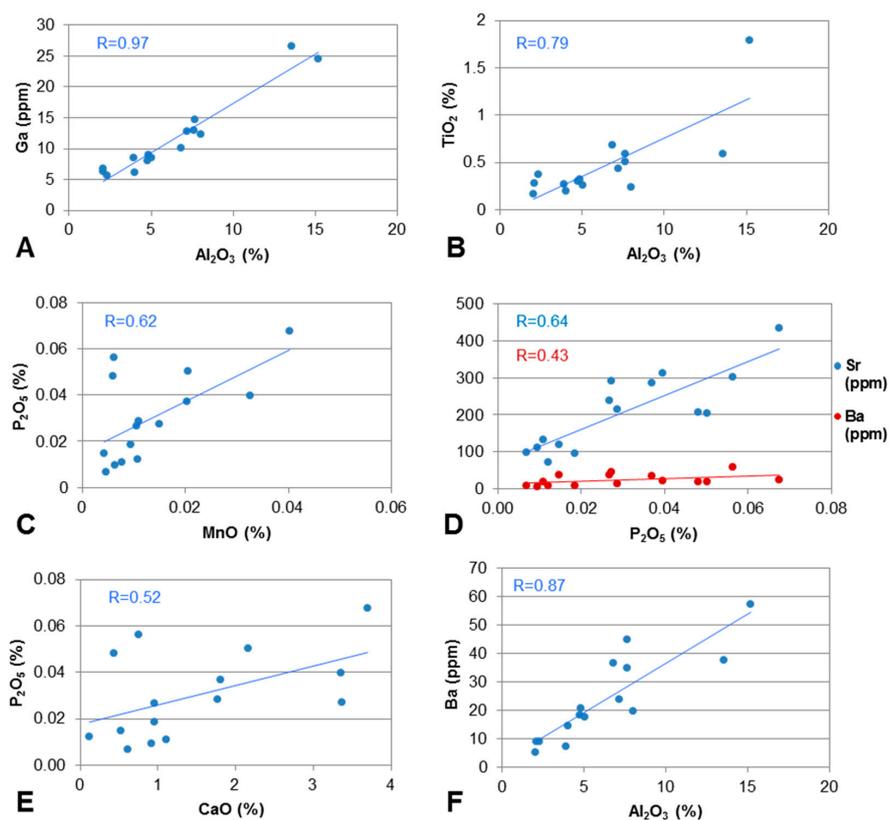
Figure 4. Correlations between selected elements in the Songzao coal samples: (**A**) Ga against Al_2O_3; (**B**) TiO_2 against Al_2O_3; (**C**) P_2O_5 against MnO; (**D**) Sr and Ba against P_2O_5; (**E**) P_2O_5 against CaO; and (**F**) Ba against Al_2O_3. Relevant correlation coefficients (R), obtained from linear regression analysis, are also shown in each case.

Group D includes MgO, MnO, Mo, Sr, Eu, CaO, Te and P_2O_5. With the exception of Mo, all the elements in this group are strongly or relatively strongly correlated with CaO, and thus have a carbonate affinity. P_2O_5 and Sr are probably associated with aluminophosphate minerals, which were detected by EDS analysis in the coals [19]. Molybdenum, although clustered in this group, also has an affinity with the sum of the abundances of pyrite and marcasite (correlation coefficient of 0.66), expressed on a whole-coal basis.

Group E includes Fe_2O_3, As, Zn, Pb, Cd, Hg, Co, Ni, Se, Sb and Bi. These elements have either no or a negative correlation with Al_2O_3 (R in the range of -0.73 to 0.39) or with ash yield (R in the range of -0.36 to 0.3). The elements in this group are mainly chalcophile elements. However, only As is significantly correlated with pyrite, having a correlation coefficient of 0.89. Hg and Se are weakly correlated with the sum of the abundances of pyrite and marcasite in the coals, with correlation coefficients of 0.32 and 0.43, respectively.

Group F includes Be, Tl and SiO_2, which do not have obvious correlation with each other. No overall correlation exists between Be and quartz (or SiO_2), although an elevated Be concentration is present in one quartz-rich coal sample (yy-11-1).

4.3. Associations of Major Elements in the Coals

The major elements in the Songzao coals are dominated by SiO_2, Al_2O_3 and Fe_2O_3 (Table 2). The main carriers of these elements are quartz, clay minerals and pyrite [19]. The concentration of TiO_2 is relatively high in the Songzao coals. EDS analysis indicates that TiO_2 occurs in the clay minerals, as anatase crystals, and as finely disseminated submicron particles of anatase or Ti-bearing phases with possibly poor crystallinity [19]. A positive correlation exists between TiO_2 and Al_2O_3 ($R = 0.79$) in the ash chemistry (Figure 4B). The TiO_2/Al_2O_3 ratio of the Songzao coal ashes ranges from 0.03 to 0.16. As discussed by Ward *et al.* [32], part of the TiO_2/Al_2O_3 ratio might be attributed to the incorporation of Ti in the aluminosilicate (e.g., kaolinite) structure. The intimate association of anatase (and fine Ti-bearing phases) and clay minerals in the Songzao coals, as noted in some cases by Zhao *et al.* [19], indicates that kaolinite and TiO_2 may have been co-precipitated. TiO_2 in some of the coals also occurs as separate masses of anatase replacing probable volcanic components [19]. The high proportions of TiO_2 in the Songzao coals may partly reflect high Ti contents in the sediment input to the original peat swamp, derived from the mafic basaltic rocks of the Kangdian Upland on the western margin of the coal basin [18]. The occurrence of the volcanic components replaced by TiO_2 also suggests that Ti can be introduced, or at least moved around, in solutions permeating through the peat/coal after deposition, perhaps as a more soluble $Ti(OH)_4$ component or as organo-metallic complexes.

Na_2O shows great variability in the Songzao coals. Several coal and non-coal samples in the Datong and Tonghua sections are high in Na_2O, which is mainly attributed to the presence of albite. High proportions of Na_2O in a few of the coal samples are also attributed to the presence of Na-rich illite and Na-I/S, rather than the more common K-illite and K-I/S in the Songzao coals [19].

High correlations of MnO-CaO ($R = 0.86$) and MnO-MgO (0.96) indicate that the MnO in the Songzao coals may be closely associated with carbonates (calcite, dolomite and ankerite). Dai *et al.* [17] noted the presence of fine-grained alabandite (MnS) (about 1 μm) of hydrothermal origin in the Songzao No. 11 coal, which was probably the most important carrier of manganese in those samples. However, alabandite was not observed in the Songzao coals during the present study. Siderite is also present in some of the coals [19], but the concentration of Mn in the siderite was below the detection limit of the SEM-EDS system used for that study.

P_2O_5 shows a positive correlation with MnO (Figure 4C). As discussed further below, P_2O_5 also shows significant correlations with Sr (Figure 4D) and Ca (Figure 4E), but no correlation with Ba (Figure 4D). This indicates that P_2O_5 mainly occurs in aluminophosphates of the goyazite and probably crandallite groups. Although no correlation exists between P_2O_5 and Ba, the presence of gorceixite was indicated by the SEM study [19]. Ba in the Songzao coals may have additional sources other than gorceixite (e.g., barite), which were not identified by either XRD or microscope studies.

4.4. Selected Elements in the Roof, Floor and Claystone Samples

The concentration of TiO_2 is as high as 4.09% in the K-bentonite band of the Tonghua section (sample th-k2b-3), much higher than that in the tonsteins (samples th-k2b-5 and yy-11-6) of the Songzao coal seam. The TiO_2/Al_2O_3 ratio has been compared with that found in volcanic rocks to identify sediments with a possible volcanic component in the coal-bearing sequences, or to indicate the possible composition of the parent magma in many studies [18,33–37]. In the study of Spears and Kanaris-Sotiriou [38], tonsteins with TiO_2/Al_2O_3 values of <0.02 and >0.07 are grouped to indicate parent magmas of acid and mafic compositions, respectively; those with values in between are thought to represent intermediate ash materials.

A comparison of the TiO_2 and Al_2O_3 percentages in the Songzao non-coal samples is potted in Figure 5A. On this diagram, the TiO_2-rich bentonite, sample th-k2b-3, plots in the mafic field while the

other two tonsteins plot between the two lines indicating TiO_2/Al_2O_3 values of 0.02 and 0.07. The key parameters for the claystones were also investigated using the magma source discrimination diagram of Winchester and Floyd [39] (Figure 5B). On this diagram, the bentonite (th-k2b-3) falls in the alkali basalt field, while the two tonsteins fall in the trachyte and basanite/nephelinite fields.

As discussed above, Zr, Nb, and Y are relatively mobile in the volcanic ash layers investigated, potentially making the use of discrimination diagrams such as that of Winchester and Floyd [39] less reliable as provenance indicators. The actual Zr/TiO_2 ratios for the claystones may also be less than those shown in the plot, due to possible contamination of the samples from the zirconia grinding mill used during sample preparation. This, coupled with decreased Zr, Nb and Y concentrations in the studied claystones due to leaching, may therefore have affected to some extent the fields in which the samples plot. Nevertheless, mafic characteristics for claystone th-k2b-3 and intermediate characteristics for claystones th-k2b-5 and yy-11-6 are confirmed by their TiO_2/Al_2O_3 ratios (Figure 5A). It is thus tentatively concluded that the bentonite and the two tonsteins were derived from mafic and alkali ashes, respectively.
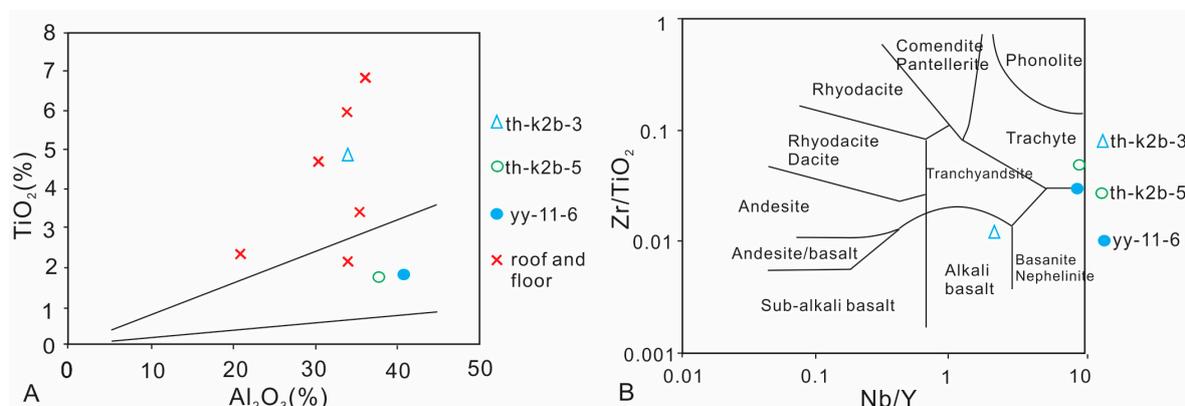
Figure 5. Plots of elements for the Songzao non-coal samples. (**A**) Comparison of TiO_2 and Al_2O_3 concentrations. The upper and lower diagonal lines represent TiO_2/Al_2O_3 values of 0.07 and 0.02, respectively. (**B**) Plot of Zr/TiO_2 against Nb/Y ratios using the magma source discrimination diagram of Winchester and Floyd [39].

As indicated in Figure 5A, the roof and floor samples generally have high TiO_2 contents. This reflects a high Ti content in the detrital sediment input from the source region, probably mafic basalts from the Kangdian Upland on the western margin of the coal basin.

Two groups of elements are enriched in the mafic K-bentonite and the alkali tonsteins, respectively, not only relative to the coal plies, but to the roof and floor samples in the respective seam sections (Figure 6). The high field strength elements, including Nb, Ta, Zr, Hf, REE and Y, are enriched in the alkali tonsteins. Another group of elements (V, Cr, Co, Cu and Ni), most of which are transition elements, are concentrated in the mafic K-bentonite band (Figure 6).

The relatively immobile elements in tonsteins are considered to be present in resistate phases, such as ilmenite (Ti) and zircon (Zr and Hf), and diagenetic minerals such as kaolinite (Al) and anatase (Ti) [40]. Spears and Rice [34] suggested that Ga and Th can be accommodated in kaolinite, and U and probably Y in zircon. Zircon in coal may also contain Nb, Ta and Th [6]. These minerals, if incorporated as volcanogenic components within the coal, may be responsible for enrichment of the immobile elements.

High concentrations of Nb, Ta, Zr, Hf and REE have been reported in alkali tonsteins, relative to silicic and mafic tonsteins [10,18]. Dai *et al.* [17] suggested that alkaline volcanic ash is responsible for the enrichment of elements such as Nb, Zr, Ga, Hf and REE in the No. 11 coal of the Songzao Coalfield, where only clayey micro-sized bands were observed.
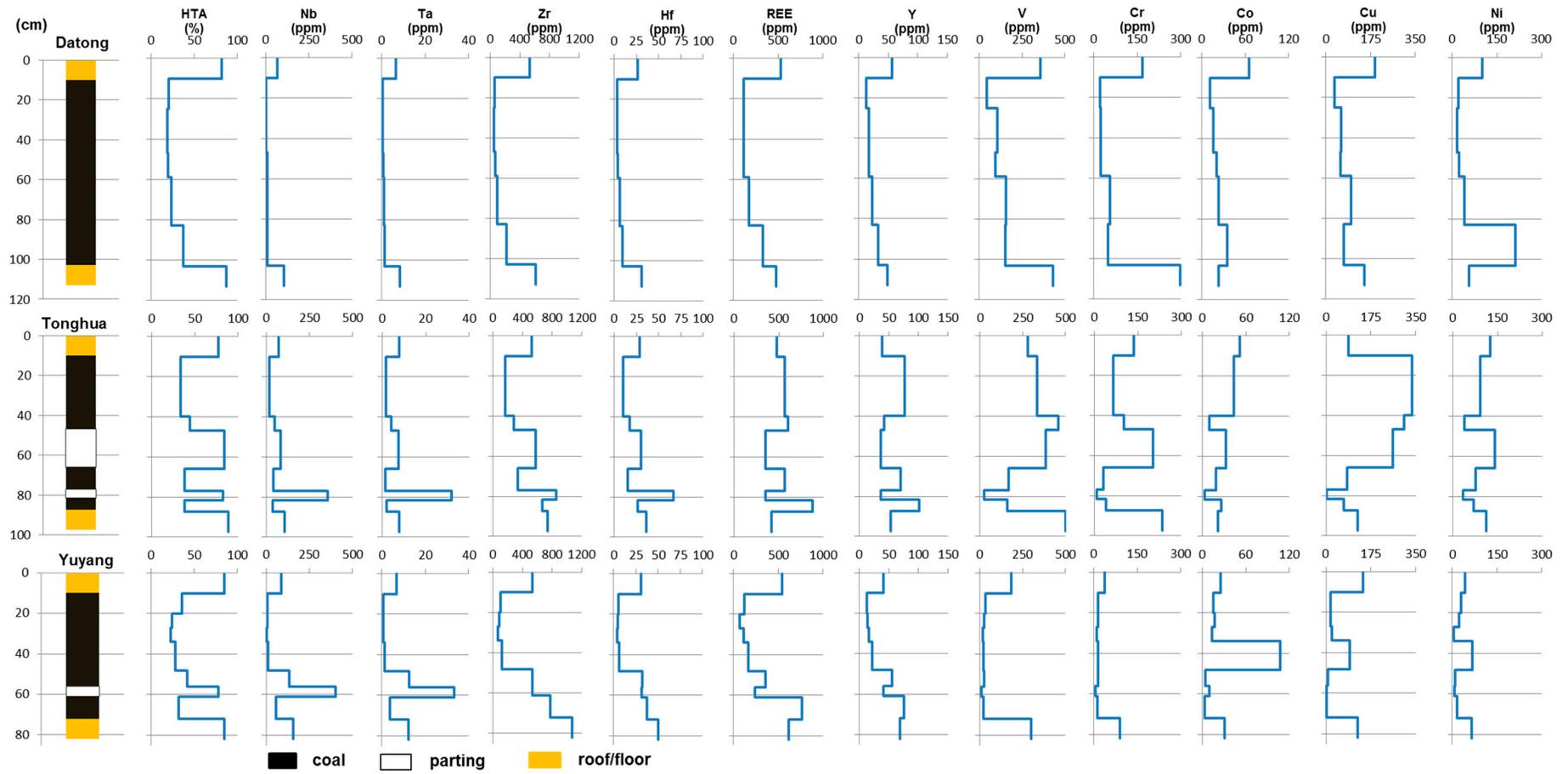
Figure 6. Plots showing vertical variation of percentage of high temperature ash and selected trace element concentrations in the Songzao seam sections.

4.5. Selected Trace Elements in Coal Samples

As indicated by the cluster analysis, many elements are associated with Al_2O_3 or the ash yield of the coals with different degrees of affinity. Apart from the ash yield, other factors may also control the concentrations of different trace elements in the different coal seams.

4.5.1. Sr and Ba

The concentration of P_2O_5 shows positive correlations with the concentrations of Sr and Ba in the coal samples ($R = 0.64$ and 0.43 respectively). The Sr and Ba in the coals probably occur in aluminophosphates (goyazite and gorceixite), also confirmed by SEM-EDS analysis for some coal samples [19]. The moderate correlation between Ba and P_2O_5 may indicate that some of the Ba had sources other than gorceixite. Some Ba also occurs in authigenic rhabdophane, as indicated by EDS analysis [19]. A significant positive correlation, however, is shown in the plot of Ba against Al_2O_3 (Figure 4F). This indicates that a large proportion of the Ba in the Songzao coals is associated with aluminosilicates, probably clay minerals, or substituting for calcium in the plagioclase structure, with only minor Ba occurring in the aluminophosphates (mainly gorceixite and rhabdophane). Alternatively, the correlation between Ba and Al_2O_3 may indicate a common source.

Additionally, the occurrence of goyazite-, gorceixite- or crandallite-group minerals and elevated concentrations of F, P and Sr in other coals and associated rocks is often indicative of volcanic input [41–43].

4.5.2. V, Cr, Cu, Co and Ni

The concentrations of V, Cr, Cu, Co and Ni are generally high in the Datong and Tonghua coals. Cu, for example, has the highest concentration in the coals, being 457, 103 and 334 ppm, respectively. These elements are also correlated with each other. The correlations among V, Cr and Cu are especially strong, with R being 0.96 for V and Cr, and 0.92 for V and Cu (Figure 7A). A significant correlation between V and Cr was also observed in coals from the Gunnedah Basin, Australia, in a study by Ward *et al.* [32], who suggested that a common magmatic source may be reflected. Glick and Davis [44] suggested that Cr may have an association with illite in a large number of US coals.

Copper in the Songzao coals has a moderate correlation with Al_2O_3 ($R = 0.47$). However, along with V and Cr, Cu shows a significant positive correlation with the sum of illite and I/S (Figure 7B) ($R = 0.88$, 0.84 and 0.76 respectively). The correlations are apparent in those samples where the proportion of illite +I/S is greater than 5% (whole coal basis). Siroquant may have difficulties in quantification of illite and I/S when in small proportions (<5%, whole coal basis), and this may account for the poor correlations between illite + I/S and these elements.
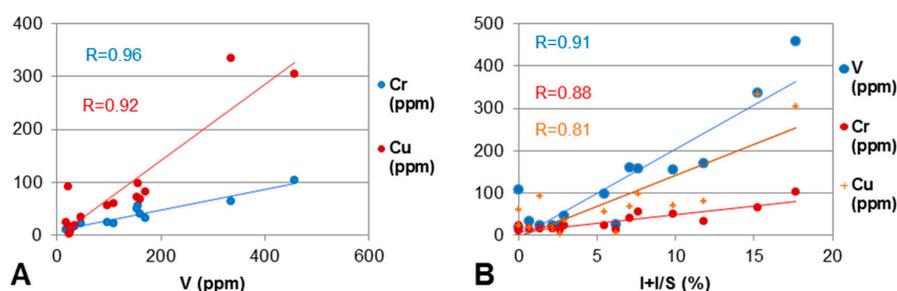
Figure 7. Correlations between selected elements in the Songzao coal samples: (**A**) Cr and Cu against V; and (**B**) V, Cr and Cu against the sum of illite and I/S, on a whole-coal basis. Relevant correlation coefficients (*R*), obtained from linear regression analysis, are also shown in each case.

Cu in coal has been reported to be associated with sulfides [45–47] and carbonates [48], and occassionally to occur as Cu sulfides and oxides [49]. Organically bound Cu has also been suggested

in some coals [50,51]. However, neither of these associations is indicated in the Songzao coals. Cu is not only associated with illite and I/S, but also appears to have a similar pattern of variation to V and Cr (Figure 7).

The correlations between V, Cr and Cu and the sum of illite and I/S may indicate a common source of clastic material supplied to the coal basin, which was in turn probably derived from the mafic basaltic rocks of the Kangdian Upland in southwestern China. Vanadium, Cr and Cu are especially concentrated in the Tonghua coals, with the coals of the upper section being more enriched in these elements than those in the lower section. This is mostly likely related to the underlying mafic bentonite. Leaching of the original mafic ash may have led to higher concentrations of these elements in the underlying coal than in coals without such an influence or affected by alkaline ashes. As physio-chemical conditions change, re-precipitation of these elements within the overlying coal layers may also occur, due to the leaching of these elements from the mafic bentonite by upwelling fluids.

4.5.3. Chalcophile Elements

The plot of As against the proportion of iron sulfides (the sum of pyrite and marcasite) shows a relatively strong and consistent correlation (Figure 8A). The correlation trend indicates the presence of approximately 0.3 ppm of As per 1% of iron sulfides, or 30 ppm of As present in the iron sulfides themselves. This ratio is comparable with that in the high sulfur Greta coals of the Sydney Basin, Australia (10 ppm in pyrite) (unpublished data), but much lower than that in the coals from the Gunnedah Basin, Australia (1000 ppm in pyrite) as discussed by Ward *et al.*, [32]. Further evaluation of Figure 8A indicates that the correlation line intersects the y (As) axis, indicating a value of 1.4 ppm As when the pyrite concentration is zero. This may be due to the presence of small proportions of organically-associated As in the coal samples. Alternatively, this may also be due to the presence of arsenate (AsO_4^{3-}), formed during pyrite oxidation during storage under ambient conditions. The presence of arsenate has been indicated by XAFS studies in a range of US bituminous coals [52,53].

As indicated in Figure 8B, a positive correlation also exists between Mo and the total iron sulfides in the coals, with a correlation coefficient of 0.66. Figure 8B shows the presence of approximately 0.2 ppm of Mo with 1% of iron sulfides, or 20 ppm of Mo present in the iron sulfides themselves. An association of Mo with iron sulfides is observed in some coal deposits [54,55] but not in others [32]. LA-ICP-MS studies of coals from the Black Warrior Basin, USA, by Diehl *et al.* [56], indicated that varying but significant concentrations of Mo (<10–582 ppm) and As (<100–27400 ppm) are present in pyrite within the coals of that basin. The results of the present study show an overall consistent relationship between As and Mo to the proportion of iron sulfides in the Songzao coals. However, there appears to be some variation in Mo concentration in these sulfides, as expressed by the scatter of individual points on the graph.

Mercury and Se are only broadly correlated with the iron sulfide content (Figure 8C,D). Both of these elements have been reported to be commonly associated with pyrite in other coals, but the degree of scatter found in the present study is relatively high. The concentration of Hg in the individual coal plies of the Songzao Coalfield is mostly in the range of 0.3 to 0.9 ppm, with the highest value being 1.1 ppm. This is much higher than the average Hg concentration of Chinese coals, which is 0.163 ppm [57]. A relatively high correlation coefficient exists between Tl and iron sulfides (Figure 8E). However, this relationship is dominated by the presence of several samples with very high iron sulfide proportions (>12.4%, on a whole coal basis). The same iron sulfide-rich coals contain the highest concentrations of Ge (Figure 8F), despite poor correlation between Ge and the iron sulfides in other coals of the samples studied.

Other chalcophile elements, such as Sb, Pb, Co, Ni, Cu and Zn, show either poor or negative correlations with total iron sulfides, although different degrees of positive correlation have also been reported in other coal deposits. This may reflect the variation of the concentrations of these elements in individual pyrite/marcasite (including Tl and Ge), or simply poor retention of those elements

in the pyrite/marcasite of the Songzao coals. Co, Ni, Cu and Zn could also be associated with the clay minerals. For example, Cu in the Songzao coals is correlated with the sum of illite and I/S, as discussed above.
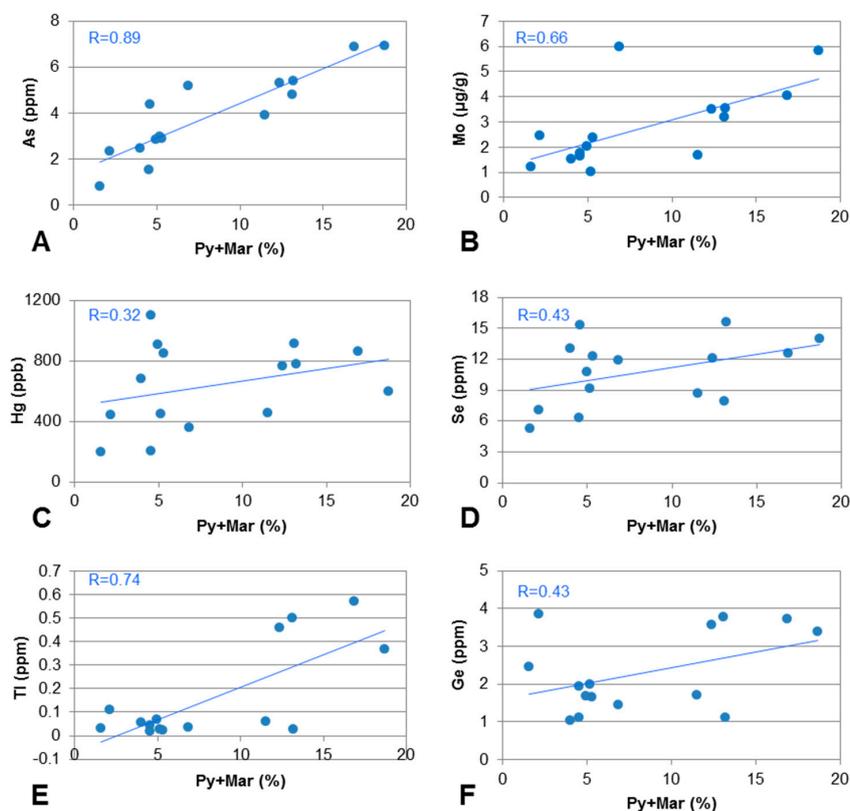
Figure 8. Correlation of selected elements (As, Mo, Hg, Se, Tl and Ge) with the sum of pyrite and marcasite in the Songzao coal samples, on a whole-coal basis: (**A**) As against iron sulfides (the sum of pyrite and marcasite); (**B**) Mo against iron sulfides; (**C**) Hg against iron sulfides; (**D**) Se against iron sulfides; (**E**) Tl against iron sulfides; and (**F**) Ge against iron sulfides. Relevant correlation coefficients (*R*), obtained from linear regression analysis, are also shown in each case.

4.5.4. Nb, Ta, Zr, Hf, Th, U and REE

Niobium, Ta, Zr, Hf, Th and U, also referred to as high field strength elements, are enriched in all the coals in the Tonghua section and two coals near the alkali tonstein band in the Yuyang section (Table 2). The variation in Zr, however, may also be derived from contamination of the coals from the zirconia grinding mill used during sample preparation.

The concentrations of Nb, Ta, Zr, Hf, REE and Y are notably higher in the coal ply (yy-11-5) overlying the alkali tonstein in the Yuyang section, and in the coal plies (th-k2b-6 and yy-11-7) under the alkali tonsteins in the Tonghua and Yuyang sections (Figure 6). It is also worth noting that the REE and Y concentrations in both the overlying and underlying coal plies are higher than those in the tonsteins of the Tonghua and Yuyang sections.

Elevated concentrations of trace elements in coals near tonsteins are relatively common and volcanic minerals or volcanic glasses are probably the sources for the elevated element concentrations in such coals [6]. For example, the enrichment of Zr, Nb, Th and Ce in coals directly above and below tonsteins in the C coal bed of the Emery Coal Field, Utah was reported by Crowley *et al.* [6]. Crowley *et al.* [6] suggested that the mechanism of enrichment for some elements in the coal was leaching of volcanic ash by groundwater and subsequent incorporation in organic matter or authigenic minerals, or, alternatively, the incorporation of volcanic ash in the original peat material. Leaching of

the volcanic ash by ground water was used by Hower *et al.* [7] to explain the high concentrations of Zr, Y and REE in the coal directly underlying a tonstein in the Fire Clay coal bed, Kentucky. Similar observations suggesting enrichment of elements due to leaching of volcanic ash beds in coals were also made by Wang [58].

Although Nb, Ta and the REE are relatively immobile in most low-temperature environments, Zielinski [40] suggested that the high leaching efficiency in acid coal-forming swamps may explain the significant mobility of these elements during the alteration of volcanic ash to tonsteins. Zielinski [40] indicated that Zr and Hf were the most resistant to mobilization. In the present study, although Nb and Ta are significantly enriched in the alkali tonsteins, no significant elevation of their concentrations was observed in the adjacent coal samples (Figure 6).

The positive correlations between the high field strength elements and Al_2O_3 in coal most likely indicate a common source, namely the original volcanic ash. In the present study, Nb was also detected in anatase by EDS in the Tonghua coals, and in fine Zr-phases (<0.5 μm), probably zircon, in the tonsteins [19]. The fine Zr-phases in the tonsteins are probably authigenic, and similar phases may also occur in the coal samples [19]. If such material is present in the coals, it may possibly have been overlooked during SEM examination due to the fine particle size. Primary minerals of volcanogenic origin (e.g., zircon) mainly made-up of these elements, however, were not observed in the coals of the present study, and thus are probably not the main carrier of the elements in question.

Although the presence of REE mineral veins in a Tonghua coal (th-k2b-4) [19] may lead to high REE concentrations, the occurrence of such minerals may not account for the elevated REE in all the coal samples adjacent to the tonsteins. The main carrier of REE in the coals is fine-grained authigenic REE-phosphates, probably rhabdophane, which is also indicated by SEM data [19].

4.6. Distribution and Affinity of REE and Y

The REY content (∑REE + Y) of the Songzao coals from the three sections ranges between 70 and 874 ppm (Table 4). The maximum REY concentration in each section appears to occur in the coal immediately above the floor strata (Table 4). The highest REY concentration in the Datong section is in the lowermost coal ply, which may be related to its high ash yield; in both the Tonghua and Yuyang sections, the coal plies near alkali tonsteins have elevated REY contents. However, all the altered volcanic ash bands have REE and Y concentrations lower than those in the respective overlying and underlying coal samples.

The correlation coefficients between the concentrations of individual REY and the ash yield are mainly in the range of 0.6 to 0.7, except for Eu, which has a correlation coefficient with ash of 0.58 (Figure 9). The REE exhibit less significant correlations with Al_2O_3 ($R = 0.4$–0.6). This indicates that the REE generally have similar mineral affinities. Ce may have a slightly greater organic affnity than the other REE. A stronger organic affinity for heavy REE has been observed in some coal deposits [59,60], while the light REE exhibit greater organic affinity in other coals [61].
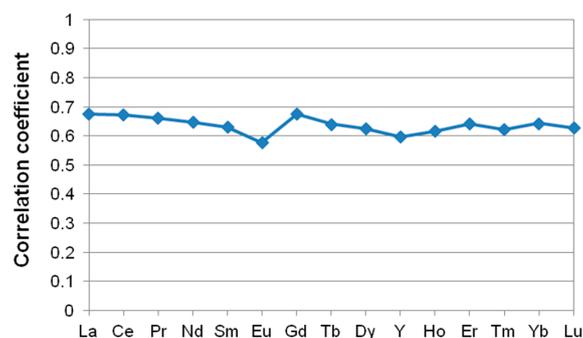
Figure 9. Correlation coefficients between mean individual REE and Y with ash yield in the Songzao coal samples.

Table 4. Rare earth elements and Y (REY) in the Songzao coal samples and associated strata (REY concentrations in ppm, on whole-coal basis).

Element	Sample														
	dt-7-0	dt-7-1	dt-7-2	dt-7-3	dt-7-4	dt-7-5	dt-7-6	th-k2b-0	th-k2b-1	th-k2b-2	th-k2b-3	th-k2b-4	th-k2b-5	th-k2b-6	th-k2b-7
La	85.56	20.33	19.49	18.38	32.03	61.68	85.92	88.63	92.56	121.1	59.46	100	58.17	151.5	68.12
Ce	187.1	43.26	36.89	38.05	61.1	125.4	172.2	194.2	203.3	239.2	115.1	206.6	117.2	316.3	131.9
Pr	24.32	5.35	4.53	4.68	6.82	14.65	21.57	22.78	24.27	27.36	16.45	24.54	13.88	39	17.82
Nd	91.54	19.59	17.81	18.4	25.51	57.94	77.68	81.41	91.4	99.71	63.58	90.02	49.82	153.4	69.01
Sm	19.43	3.59	3.73	3.43	4.4	10.24	12.66	10.67	18.37	19.69	10.7	16.85	10.38	32.14	16.1
Eu	4.96	0.88	1.05	0.68	0.82	2.08	2.59	1.44	3.73	3.26	2.38	3.75	2.65	5.81	2.68
Gd	23.72	3.05	4	3.37	5.08	9.95	20.11	16.8	19.17	20.19	16.37	15.99	19.48	25.83	22.52
Tb	2.72	0.46	0.63	0.52	0.74	1.29	2.29	1.73	2.78	2.2	2.4	2.64	2.9	3.5	2.98
Dy	14.52	2.58	3.37	3.02	4.25	6.6	13.08	10.29	14.99	10.45	13.74	14.32	17.82	18.98	15.28
Y	56.21	12.85	17.64	16.87	23.29	32.44	48.98	38.27	77.11	42.29	36.78	70.26	36.54	101.4	52.67
Ho	2.79	0.51	0.7	0.61	0.92	1.33	2.48	1.98	3.17	1.92	2.51	3.19	3.44	3.92	2.66
Er	7.36	1.41	1.8	1.7	2.59	3.87	6.96	5.72	8.36	5.49	6.48	8.71	9.26	10.4	6.78
Tm	0.99	0.2	0.24	0.25	0.35	0.51	0.96	0.77	1.23	0.73	0.76	1.36	1.21	1.45	0.88
Yb	6.45	1.27	1.48	1.53	2.26	3.42	5.75	4.69	7.27	4.76	4.71	8.19	7.34	8.79	5.43
Lu	0.96	0.19	0.21	0.24	0.32	0.52	0.88	0.67	1.07	0.67	0.64	1.29	1.05	1.36	0.77
REY	529	116	114	112	170	332	474	480	569	599	352	568	351	874	416
REO	634	139	136	134	205	398	569	576	683	719	422	681	421	1049	499
REO$_a$	777	675	747	691	884	1124	652	742	2115	1645	501	1861	512	2866	562
Eu/Eu *	1.07	1.24	1.27	0.93	0.8	0.96	0.73	0.48	0.93	0.76	0.81	1.07	0.81	0.95	0.64
Ce/Ce *	0.93	0.94	0.9	0.93	0.94	0.95	0.91	0.98	0.98	0.95	0.84	0.95	0.94	0.94	0.86
Y/Y *	0.67	0.85	0.87	0.94	0.9	0.83	0.65	0.64	0.85	0.71	0.47	0.79	0.35	0.89	0.62
(La/Lu)$_N$	0.95	1.13	0.98	0.81	1.07	1.27	1.05	1.41	0.93	1.92	0.997	0.83	0.59	1.19	0.95
(La/Sm)$_N$	0.66	0.85	0.78	0.8	1.09	0.9	1.02	1.25	0.76	0.92	0.83	0.89	0.84	0.71	0.63
(Gd/Lu)$_N$	2.08	1.34	1.58	1.17	1.34	1.62	1.93	2.11	1.51	2.52	2.17	1.04	1.56	1.6	2.47
Type	H-M	L-M	H-M	H-M	L	L-M	L	L	H-M	L-M	M	M	M	L-M	H-M

Table 4. *Cont.*

Element	Sample								
	yy-11-0	**yy-11-1**	**yy-11-2**	**yy-11-3**	**yy-11-4**	**yy-11-5**	**yy-11-6**	**yy-11-7**	**yy-11-8**
La	98.11	24.25	11.69	20.84	30.15	69.42	44.3	160.9	122.1
Ce	215.3	47.44	23.26	41	60.41	128.6	83.98	304.5	244.6
Pr	25.64	4.75	2.56	4.5	6.91	13.99	8.33	32.81	24.22
Nd	94.73	15.57	9.08	15	24.36	47.5	26.09	114	70.8
Sm	17.4	2.69	1.81	2.75	4.28	8.35	5.03	19.46	12.26
Eu	3.15	0.4	0.28	0.37	0.56	1.09	0.81	2.18	2.69
Gd	20.98	2.78	1.54	2.38	4.53	8.92	9.93	17.58	26.77
Tb	2.02	0.36	0.32	0.46	0.67	1.59	1.22	2.84	3.11
Dy	11.04	2.16	2.13	2.72	4.05	9.54	7.45	15.31	18.37
Y	41.25	12.77	14.24	15.65	21.85	55.61	40.32	75.1	68.58
Ho	2.09	0.47	0.48	0.58	0.85	2.09	1.48	3.03	3.39
Er	6.11	1.43	1.37	1.64	2.48	5.88	4.19	8.32	9.75
Tm	0.85	0.21	0.21	0.23	0.35	0.82	0.54	1.2	1.42
Yb	5.33	1.47	1.3	1.4	2.2	5	3.25	7.42	9.52
Lu	0.78	0.22	0.21	0.22	0.33	0.74	0.44	1.13	1.3
REY	545	117	70	110	164	359	237	766	619
REO	654	140	85	132	197	431	285	919	743
REO$_a$	768	390	353	545	835	1044	365	2917	871
Eu/Eu *	0.76	0.68	0.78	0.67	0.6	0.59	0.49	0.55	0.63
Ce/Ce *	0.98	1	0.97	0.96	0.95	0.94	0.99	0.95	1.02
Y/Y *	0.65	0.96	1.07	0.95	0.9	0.95	0.92	0.84	0.66
(La/Lu)$_N$	1.35	1.19	0.61	1.01	0.98	0.998	1.07	1.52	0.999
(La/Sm)$_N$	0.85	1.35	0.97	1.13	1.06	1.25	1.32	1.24	1.49
(Gd/Lu)$_N$	2.28	1.08	0.63	0.91	1.16	1.01	1.89	1.31	1.73
Type	L-M	L	H	L	H	H	L	L	H

REY, sum of rare earth elements and yttrium; REO, sum of oxides of rare earth elements and yttrium; Subscript a indicates value on ash basis; Subscript N indicates values normalized by the average REE content of Upper Continental Crust (Taylor and McLennan, 1985). Eu/Eu * = $2Eu_N/(Sm_N + Gd_N)$; Ce/Ce * = $2Ce_N/(La_N + Pr_N)$; Y/Y * = $2Y/(Dy_N + Ho_N)$.

High correlation coefficients (0.71 to 0.85) exist between the concentrations of individual REY and P_2O_5. This indicates that some REY probably occur as phosphate phases, such as rhabdophane. Thus, the high REE concentration of the coal underlain by the bentonite in the Tonghua section may be attributed to authigenic rhabdophane and REE-hydroxides/oxyhydroxides and REE-carbonates occurring as fracture infillings in the coal. The low REE concentrations in the partings are probably due to leaching by groundwater during parting formation [61,62].

The REY concentrations in each coal and non-coal sample were also normalized against the Upper Continental Crust (UCC) [63], in order to obtain a more clear indication of the distribution patterns (Figure 10). Seredin and Dai [64] classified the distribution of REY into three enrichment types, namely L-type (light REY type enrichment), M-type (medium REY enrichment type) and H-type (heavy REY enrichment type). All the three types, as well as a mixed type, of REE enrichment based on this classification occur in the Songzao coal and non-coal samples (Table 4).

The REY enrichment in most of the Datong and Tonghua coals is dominated by a mixed type, either L-M or H-M type. The Yuyang coals have either L-type or H-type enrichment. Nevertheless, the dominance of M-type for the Datong and Tonghua coals indicates a different REY source from that of the Yuyang coals. As discussed by Seredin and Dai [64], an M-type of REY plot, normalized to the UCC, may be due to the circulation of acid natural waters, including acid hydrothermal solutions with high REY concentrations, in the coal basin.

Despite the diversity in the enrichment types, relatively flat REY distribution patterns tend to exist for the coals in the upper part of the Datong (Figure 10A) and Yuyang (Figure 10E) sections. The non-coal samples, including the claystone partings, show no obvious Ce anomalies, pronounced negative Y anomalies, and either no obvious or negative Eu anomalies (Figure 10B,D,F).
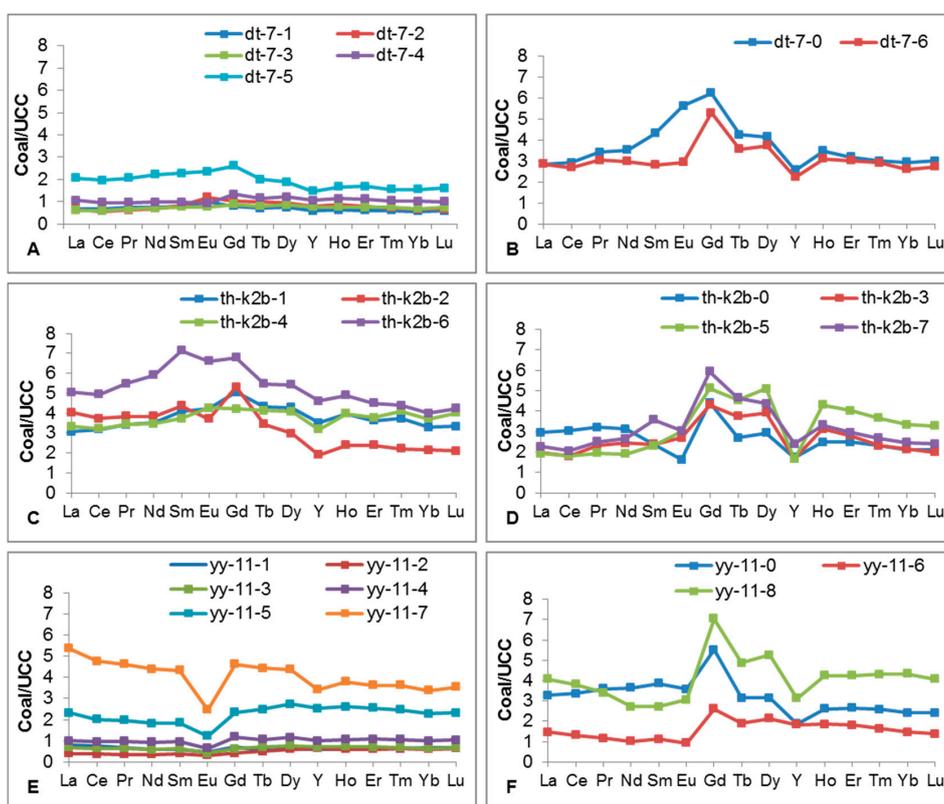
Figure 10. Distribution patterns of REE in the three seam sections. REE are normalized to Upper Continental Crust (UCC) (data from [63]). (**A**) Coal samples in the Datong section; (**B**) rock samples in the Datong section; (**C**) coal samples in the Tonghua section; (**D**) rock samples in the Tonghua section; (**E**) coal samples in the Yuyang section; and (**F**) rock samples in the Yuyang section.

4.7. Potential Industrial Value of REY in Coal Ashes

The average REY concentrations in the Datong, Tonghua and Yuyang coals ashes are 704 µg/g (or 0.84% REY_2O_3), 1737 µg/g (or 2.09% REY_2O_3), and 911 µg/g (or 1.09% REY_2O_3), respectively. The REY concentrations of the latter two coal ashes are higher than the typical REY cut-off-grade (0.1% REY_2O_3) in coal combustion wastes for by-product recovery [64].

In order to evaluate the potential industrial value of REY in the Songzao coal ashes, the $REY_{def, rel}$-Coutl graph proposed by Seredin and Dai [64] is also adopted in the present study (Figure 11). The *y*-axis is the percentage of critical elements (Nd, Eu, Tb, Dy, Y and Er) in the total REY ($REY_{def, rel}$), and the *x*-axis is the ratio of the amount of critical REY metals to the relative amount of excessive REY (Ce, Ho, Tm, Yb and Lu) in total REY. The Songzao coal ashes fall mostly in area II of the graph, which indicates that the coal ashes can be regarded as promising REY raw materials.
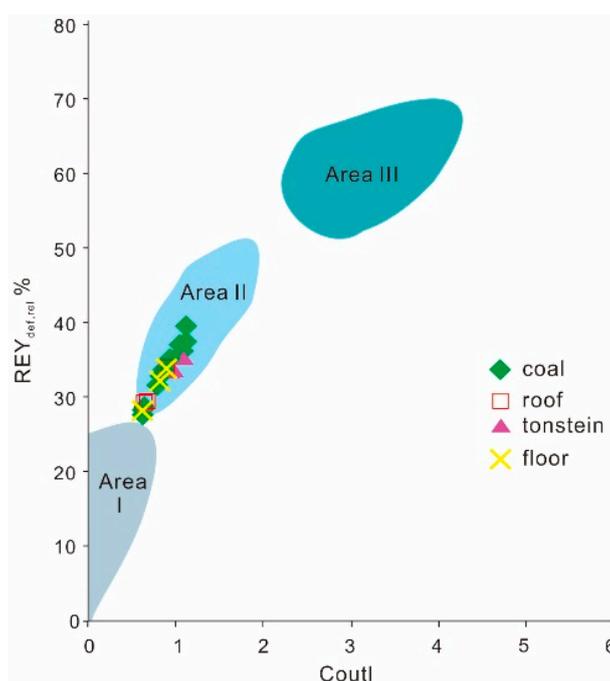
Figure 11. $REY_{def, rel}$-Coutl plot for the ashes of Songzao coals and associated rocks: Area I, unpromising; Area II, promising; and Area III, highly promising (adapted from [64]).

5. Conclusions

The geochemistry of coals from the Songzao Coalfield has been affected by the adjacent tonstein or K-bentonite bands. Coals near the alkali tonsteins in the Tonghua and Yuyang sections are high in Nb, Ta, Hf, Ga, Th, U, REE and Y. Relative to mafic and felsic volcanic ashes, alkaline volcanic ash is enriched with REE and Y, and tends to lead to elevated REE and Y concentrations in the adjacent coals. Both of the coals occurring near the alkaline tonsteins in the Tonghua and Yuyang sections are enriched with REE and Y, which may be attributed to: (1) abundant fine-grained authigenic rhabdophane in the coal, which was probably precipitated from leachates derived from the overlying bentonite; and (2) REE-hydroxides/oxyhydroxides and REE-carbonates occurring as fracture infillings in the coal, which probably crystallized from ascending hydrothermal fluids carrying high REE concentrations.

Coal samples overlying the mafic bentonite in the Tonghua section are high in TiO_2, V, Cr, Zn and Cu. Leaching of the original mafic ash may have led to higher concentrations of these elements in the adjacent coals than in coals without such influence, or in coals affected by alkaline ashes. The TiO_2 mainly occurs as anatase, poorly-crystallized Ti-phases, and kaolinite in some of the coal and claystone samples.

The coals in the Datong section, which have neither visible tonstein layers nor obvious volcanogenic minerals, have high concentrations of TiO_2, V, Cr, Ni, Cu and Zn in intervals between coals affected by mafic and alkaline volcanic ashes. This is consistent with the suggestion that a common source material was supplied to the coal basin, derived from the mafic basaltic rocks of the Kangdian Upland to the west.

In the Songzao coals, only As and Mo show positive correlations with iron sulfides. No definitive correlations have been found between other chalcophile trace elements (e.g., Sb, Pb, Co, Ni, Cu and Zn) and iron sulfides. This may reflect wide variations of the concentrations of those elements in individual pyrite/marcasite components (including Tl and Ge), or simply poor retention of these elements in the pyrite/marcasite of the Songzao coals. Lead, Cu, Sn and Sb are positively correlated with Al_2O_3, rather than pyrite, probably indicating a common source for those elements.

Author Contributions: Lei Zhao carried out this project in partial fulfillment of her PhD program at the University of New South Wales, Australia, under the supervision of Colin Ward, co-supervised by David French, and Ian Graham. Colin Ward, David French, and Ian Graham have provided major contributions to the design of the work and gave extensive suggestions on data analyses and interpretation, as well as on the English language editing of the paper.

Conflicts of Interest: The authors declare no conflict of interest.

References

1. Swaine, D.J. *Trace Elements in Coal*; Butterworths: London, UK, 1990; p. 278.

2. Kolker, A.; Finkelman, R.B. Potentially hazardous elements in coal: Modes of occurrence and summary of concentration data for coal components. *Coal Prep.* **1998**, *19*, 133–157. [CrossRef]

3. Seredin, V.V.; Finkelman, R.B. Metalliferous coals: A review of the main genetic and geochemical types. *Int. J. Coal Geol.* **2008**, *76*, 253–289. [CrossRef]

4. Bouška, V. *Geochemistry of Coal*; Elsevier: Amsterdam, The Nederland, 1981; p. 284.

5. Hower, J.C.; Rimmer, S.M.; Bland, A.E. Geochemistry of the Blue Gem coal bed, Knox County, Kentucky. *Int. J. Coal Geol.* **1991**, *18*, 211–231. [CrossRef]

6. Crowley, S.S.; Stanton, R.W.; Ryer, T.A. The effects of volcanic ash on the maceral and chemical composition of the C coal bed, Emery Coal Field, Utah. *Org. Geochem.* **1989**, *14*, 315–331. [CrossRef]

7. Hower, J.C.; Ruppert, L.F.; Eble, C.F. Lanthanide, yttrium, and zirconium anomalies in the Fire Clay coal bed, eastern Kentucky. *Int. J. Coal Geol.* **1999**, *39*, 141–153. [CrossRef]

8. Zhou, Y.; Tang, D.; Ren, Y. Characteristics of zircons from volcanic ash-derivd tonsteins in Late Permian coalfields of eastern Yunnan, China. *Acta Sedimentol. Sin.* **1992**, *10*, 28–38. (In Chinese)

9. Zhou, Y.; Ren, Y.; Tang, D.; Bohor, B. Characteristics of zircons from volcanic ash-derived tonsteins in Late Permian coal fields of eastern Yunnan, China. *Int. J. Coal Geol.* **1994**, *25*, 243–264. [CrossRef]

10. Zhou, Y.; Bohor, B.F.; Ren, Y. Trace element geochemistry of altered volcanic ash layers (tonsteins) in Late Permian coal-bearing formations of eastern Yunnan and western Guizhou provinces, China. *Int. J. Coal Geol.* **2000**, *44*, 305–324. [CrossRef]

11. Zhou, Y.; Ren, Y.; Bohor, B.F. Origin and distribution of tonsteins in Late Permian coal seams of southwestern China. *Int. J. Coal Geol.* **1982**, *2*, 49–77. [CrossRef]

12. Zhou, Y.; Ren, Y. Element geochemistry of volcanic ash derived tonsteins in Late Permian coal-bearing formation of eastern Yunnan and western Guizhou, China. *Acta Sedimentol. Sin.* **1994**, *12*, 123–132. (In Chinese)

13. Zhou, Y.P. The alkali pyroclastic tonsteins of early stage of Late Permian age in southwestern China. *Coal Geol. Explor.* **1999**, *27*, 5–9. (In Chinese)

14. Dai, S.; Zhou, Y.; Zhang, M.; Wang, X.; Wang, J.; Song, X.; Jiang, Y.; Luo, Y.; Song, Z.; Yang, Z.; *et al*. A new type of Nb(Ta)-Zr(Hf)-REE-Ga polymetallic deposit in the Late Permian coal-bearing strata, eastern Yunnan, southwestern China: Possible economic significance and genetic implications. *Int. J. Coal Geol.* **2010**, *83*, 55–63. [CrossRef]

15. Dai, S.; Chekryzhov, I.Y.; Seredin, V.V.; Nechaev, V.P.; Graham, I.T.; Hower, J.C.; Ward, C.R.; Ren, D.; Wang, X. Metalliferous coal deposits in east Asia (Primorye of Russia and south China): A review of geodynamic controls and styles of mineralization. *Gondwana Res.* **2015**, in press. [CrossRef]

16. Seredin, V.V.; Dai, S.; Sun, Y.; Chekryzhov, I.Y. Coal deposits as promising sources of rare metals for alternative power and energy-efficient technologies. *Appl. Geochem.* **2013**, *31*, 1–11. [CrossRef]

17. Dai, S.; Zhou, Y.; Ren, D.; Wang, X.; Li, D.; Zhao, L. Geochemistry and mineralogy of the Late Permian coals from the Songzao Coalfield, Chongqing, southwestern China. *Sci. China Ser. D Earth Sci.* **2007**, *50*, 678–688. [CrossRef]

18. Dai, S.; Wang, X.; Zhou, Y.; Hower, J.C.; Li, D.; Chen, W.; Zhu, X.; Zou, J. Chemical and mineralogical compositions of silicic, mafic, and alkali tonsteins in the Late Permian coals from the Songzao Coalfield, Chongqing, southwest China. *Chem. Geol.* **2011**, *282*, 29–44. [CrossRef]

19. Zhao, L.; Ward, C.R.; French, D.; Graham, I.T. Mineralogical composition of Late Permian coal seams in the Songzao Coalfield, southwestern China. *Int. J. Coal Geol.* **2013**, *116–117*, 208–226. [CrossRef]

20. Li, W. A preliminary evaluation of coal resources in the Songzao Coalfield. *Inf. Sci. Technol. Econ.* **2007**, *17*, 148–150, (In Chinese).

21. Dai, S.; Wang, X.; Chen, W.; Li, D.; Chou, C.-L.; Zhou, Y.; Zhu, C.; Li, H.; Zhu, X.; Xing, Y.; *et al*. A high-pyrite semianthracite of Late Permian age in the Songzao Coalfield, southwestern China: Mineralogical and geochemical relations with underlying mafic tuffs. *Int. J. Coal Geol.* **2010**, *83*, 430–445. [CrossRef]

22. China Coal Geology Bureau. *Sedimentary Environments and Coal Accumulation of Late Permian Coal Formation in Western Guizhou, Southern Sichuan, and Eastern Yunnan, China*; Chongqing University Press: Chongqing, China, 1996; p. 216. (In Chinese)

23. Standards Australia. *Coal and Coke—Analysis and Testing Part 3: Proximate Analysis of Higher Rank Coal. Australian Standard 1038.22*; Standards Australia: Strathfield, Australia, 2000.

24. Li, X.; Dai, S.; Zhang, W.; Li, T.; Zheng, X.; Chen, W. Determination of As and Se in coal and coal combustion products using closed vessel microwave digestion and collision/reaction cell technology (CCT) of inductively coupled plasma mass spectrometry (ICP-MS). *Int. J. Coal Geol.* **2014**, *124*, 1–4. [CrossRef]

25. Beijing Research Institute of Coal Chemistry. *Chinese National Standard GB/T 4633-1997, Determination of Fluorine in Coal*; Standand Press of China: Beijing, China, 1997.

26. American Society for Testing and Materials (ASTM). *ASTM Standard D388. Classification of Coals By Rank*; ASTM International: West Conshohocken, PA, USA, 2012.

27. Lyons, P.C.; Spears, D.A.; Outerbridge, W.F.; Congdon, R.D.; Evans, H.T. Euramerican tonsteins: Overview, magmatic origin, and depositional-tectonic implications. *Palaeogeogr. Palaeoclimatol. Palaeoecol.* **1994**, *106*, 113–134. [CrossRef]

28. Spears, D.A. The origin of tonsteins, an overview, and links with seatearths, fireclays and fragmental clay rocks. *Int. J. Coal Geol.* **2012**, *94*, 22–31. [CrossRef]

29. Ketris, M.P.; Yudovich, Y.E. Estimations of clarkes for carbonaceous biolithes: World averages for trace element contents in black shales and coals. *Int. J. Coal Geol.* **2009**, *78*, 135–148. [CrossRef]

30. Finkelman, R.B. Modes of occurrence of environmentally-sensitive trace elements in coal. In *Environmental Aspect of Trace Elements in Coal*; Swaine, D.J., Goodarzi, F., Eds.; Kluwer Academic Publishers: Amsterdam, The Nederland, 1995.

31. Ren, D.; Zhao, F.; Dai, S.; Zhang, J.; Luo, K. *Geochemistry of Trace Elements in Coal*; Science Press: Beijing, China, 2006; p. 556. (In Chinese)

32. Ward, C.R.; Spears, D.A.; Booth, C.A.; Staton, I.; Gurba, L.W. Mineral matter and trace elements in coals of the Gunnedah Basin, New South Wales, Australia. *Int. J. Coal Geol.* **1999**, *40*, 281–308. [CrossRef]

33. Price, N.B.; Duff, P.M.D. Mineralogy and chemistry of tonsteins from Carboniferous sequences in Great Britain. *Sedimentology* **1969**, *13*, 45–69. [CrossRef]

34. Spears, D.A.; Rice, C.M. An Upper Carboniferous tonstein of volcanic origin. *Sedimentology* **1973**, *20*, 281–294. [CrossRef]

35. Spears, D.A.; Kanaris-Sotiriou, R. Titanium in some Carboniferous sediments from Great Britain. *Geochim. Cosmochim. Acta.* **1976**, *40*, 345–351. [CrossRef]

36. Addison, R.; Harrison, R.K.; Land, D.H.; Young, B.R.; Davis, A.E.; Smith, T.K. Volcanogenic tonsteins from Tertiary coal measures, east Kalimantan, Indonesia. *Int. J. Coal Geol.* **1983**, *3*, 1–30. [CrossRef]

37. Burger, K.; Zhou, Y.; Ren, Y. Petrography and geochemistry of tonsteins from the 4th Member of the Upper Triassic Xujiahe Formation in southern Sichuan province, China. *Int. J. Coal Geol.* **2002**, *49*, 1–17. [CrossRef]

38. Spears, D.A.; Kanaris-Sotiriou, R. A geochemical and mineralogical investigation of some British and other European tonsteins. *Sedimentology* **1979**, *26*, 407–425. [CrossRef]

39. Winchester, J.A.; Floyd, P.A. Geochemical discrimination of different magma series and their differentiation products using immobile elements. *Chem. Geol.* **1977**, *20*, 325–343. [CrossRef]

40. Zielinski, R.A. Element mobility during alteration of silicic ash to kaolinite-a study of tonstein. *Sedimentology* **1985**, *32*, 567–579. [CrossRef]

41. Brownfield, M.E.; Affolter, R.H.; Cathcart, J.D.; Johnson, S.Y.; Brownfield, I.K.; Rice, C.A. Geologic setting and characterization of coals and the modes of occurrence of selected elements from the Franklin coal zone, Puget Group, John Henry No. 1 mine, King County, Washington, USA. *Int. J. Coal Geol.* **2005**, *63*, 247–275. [CrossRef]

42. Rao, P.D.; Walsh, D.E. Nature and distribution of phosphorus minerals in Cook Inlet coals, Alaska. *Int. J. Coal Geol.* **1997**, *33*, 19–42. [CrossRef]

43. Zhao, L.; Ward, C.R.; French, D.; Graham, I.T. Mineralogy of the volcanic-influenced Great Northern coal seam in the Sydney Basin, Australia. *Int. J. Coal Geol.* **2012**, *94*, 94–110. [CrossRef]

44. Glick, D.C.; Davis, A. Variability in the inorganic element content of U.S. coals including results of cluster analysis. *Org. Geochem.* **1987**, *11*, 331–342. [CrossRef]

45. Spears, D.A.; Martinez-Tarazona, M.R. Geochemical and mineralogical characteristics of a power station feed-coal, Eggborough, England. *Int. J. Coal Geol.* **1993**, *22*, 1–20. [CrossRef]

46. Querol, X.; Cabrera, L.; Pickel, W.; López-Soler, A.; Hagemann, H.W.; Fernández-Turiel, J.L. Geological controls on the coal quality of the Mequinenza subbituminous coal deposit, northeast Spain. *Int. J. Coal Geol.* **1996**, *29*, 67–91. [CrossRef]

47. Kolker, A. Minor element distribution in iron disulfides in coal: A geochemical review. *Int. J. Coal Geol.* **2012**, *94*, 32–43. [CrossRef]

48. Dai, S.; Chou, C.-L.; Yue, M.; Luo, K.; Ren, D. Mineralogy and geochemistry of a Late Permian coal in the Dafang Coalfield, Guizhou, China: Influence from siliceous and iron-rich calcic hydrothermal fluids. *Int. J. Coal Geol.* **2005**, *61*, 241–258. [CrossRef]

49. Finkelman, R.B. *Mode of Occurrence of Trace Elements in Coal*; University of Maryland: College Park, MD, USA, 1980.

50. Miller, R.N.; Given, P.H. The association of major, minor and trace inorganic elements with lignites. I. Experimental approach and study of a North Dakota lignite. *Geochim. Cosmochim. Acta* **1986**, *50*, 2033–2043. [CrossRef]

51. Querol, X.; Klika, Z.; Weiss, Z.; Finkelman, R.B.; Alastuey, A.; Juan, R.; López-Soler, A.; Plana, F.; Kolker, A.; Chenery, S.R.N. Determination of element affinities by density fractionation of bulk coal samples. *Fuel* **2001**, *80*, 83–96. [CrossRef]

52. Huggins, F.E.; Shah, N.; Zhao, J.; Lu, F.; Huffman, G.P. Nondestructive determination of trace element speciation in coal and coal ash by XAFS spectroscopy. *Energy Fuels* **1993**, *7*, 482–489. [CrossRef]

53. Kolker, A.; Huggins, F.E.; Palmer, C.A.; Shah, N.; Crowley, S.S.; Huffman, G.P.; Finkelman, R.B. Mode of occurrence of arsenic in four US coals. *Fuel Proc. Technol.* **2000**, *63*, 167–178. [CrossRef]

54. Lindahl, P.C.; Finkelman, R.B. Factors influencing major, minor, and trace element variations in U.S. Coals. In *Mineral Matter and Ash in Coal*; Vorres, K.S., Ed.; American Chemical Society: Washington, DC, USA, 1986; Volume 301, pp. 61–69.

55. Spears, D.A.; Zheng, Y. Geochemistry and origin of elements in some UK coals. *Int. J. Coal Geol.* **1999**, *38*, 161–179. [CrossRef]

56. Diehl, S.F.; Goldhaber, M.B.; Hatch, J.R. Modes of occurrence of mercury and other trace elements in coals from the Warrior field, Black Warrior Basin, northwestern Alabama. *Int. J. Coal Geol.* **2004**, *59*, 193–208. [CrossRef]

57. Dai, S.; Ren, D.; Chou, C.-L.; Finkelman, R.B.; Seredin, V.V.; Zhou, Y. Geochemistry of trace elements in Chinese coals: A review of abundances, genetic types, impacts on human health, and industrial utilization. *Int. J. Coal Geol.* **2012**, *94*, 3–21. [CrossRef]

58. Wang, X. Geochemistry of Late Triassic coals in the Changhe mine, Sichuan Basin, southwestern China: Evidence for authigenic lanthanide enrichment. *Int. J. Coal Geol.* **2009**, *80*, 167–174. [CrossRef]

59. Eskenazy, G.M. Aspects of the geochemistry of rare earth elements in coal: An experimental approach. *Int. J. Coal Geol.* **1999**, *38*, 285–295. [CrossRef]

60. Dai, S.; Zou, J.; Jiang, Y.; Ward, C.R.; Wang, X.; Li, T.; Xue, W.; Liu, S.; Tian, H.; Sun, X.; *et al.* Mineralogical and geochemical compositions of the Pennsylvanian coal in the Adaohai mine, Daqingshan coalfield, Inner Mongolia, China: Modes of occurrence and origin of diaspore, gorceixite, and ammonian illite. *Int. J. Coal Geol.* **2012**, *94*, 250–270. [CrossRef]

61. Dai, S.; Li, D.; Chou, C.-L.; Zhao, L.; Zhang, Y.; Ren, D.; Ma, Y.; Sun, Y. Mineralogy and geochemistry of boehmite-rich coals: New insights from the haerwusu surface mine, Jungar Coalfield, Inner Mongolia, China. *Int. J. Coal Geol.* **2008**, *74*, 185–202. [CrossRef]

62. Dai, S.; Ren, D.; Chou, C.-L.; Li, S.; Jiang, Y. Mineralogy and geochemistry of the No. 6 coal (Pennsylvanian) in the Junger coalfield, Ordos Basin, China. *Int. J. Coal Geol.* **2006**, *66*, 253–270. [CrossRef]

63. Taylor, S.R.; McLennan, S.M. *The Continental Crust: Its Composition and Evolution*; Blackwell: Oxford, UK, 1985; p. 312.

64. Seredin, V.V.; Dai, S. Coal deposits as potential alternative sources for lanthanides and yttrium. *Int. J. Coal Geol.* **2012**, *94*, 67–93. [CrossRef]

65. Zhao, L. Mineralogy and geochemistry of Permian coal seams of the Sydney Basin, Australia, and the Songzao Coalfield, SW China. Ph.D. Thesis, University of New South Wales, Australia, 2012, unpublished.